

NUMERICAL INVESTIGATION OF PARTICLE INHALATION FROM AMBIENT ENVIRONMENT AND DEPOSITION IN HUMAN NASAL CAVITY USING AN INTEGRATED MANIKIN MODEL

Xiangdong LI¹, Qinjiang GE¹ and Jiyuan TU^{*1,2}

¹ School of Aerospace, Mechanical and Manufacturing Engineering, RMIT University, Victoria 3083, AUSTRALIA

² Institute of Nuclear and New Energy Technology, Tsinghua University, PO Box 1021, Beijing 100084, China

*Corresponding author, E-mail address: jiyuan.tu@rmit.edu.au

ABSTRACT

Particle inhalation from the ambient environment and particle deposition in the respiratory tracts are numerically investigated using an integrated breathing human manikin which includes detailed facial features as well as nasal cavity, laryngopharynx and trachea. Visualized and quantitative results including the airflow field, particle tracks and particle inhalation and deposition patterns are obtained. Compared with the previous studies which dealt with particle inhalation and deposition separately, this integrated method provides a comprehensive method for assessment of health risk associated with particle inhalation since it make it possible to trace particles from their source in the environment into their deposition locations in the respiratory tracts. More importantly, this method eliminates the information loss of velocity profile at the nostrils, which leads to a more accurate prediction.

NOMENCLATURE

| | |
|---------------|---|
| ρ | density |
| \bar{U} | velocity |
| μ | viscosity |
| μ_t | turbulent viscosity |
| δ_{ij} | Kronecker delta |
| m_p | particle mass |
| \bar{U}_p | particle velocity |
| d_p | particle diameter |
| A_p | particle projected area in the flow direction |

INTRODUCTION

Prevention of diseases or adverse health responses associated with inhalation of airborne particles is an important consideration of occupational health and safety in many industrial fields. Since the pathological change caused by particle inhalation is associated with the particle deposition in the respiratory system, the particle transport and deposition patterns in human respiratory tracts have been attached a great importance and has been intensively investigated. Since the 1990s, numerical methods based on computed tomography (CT) technology and computational fluid dynamics (CFD) have been widely employed in the investigations (Anthony and Flynn, 2006; Baldwin and Maynard, 1998; Doorly, Taylor, et al., 2008),

which has brought about an elaborate and visualized description of airflow and particle transport as well as the particle deposition pattern in human respiratory tracts.

However, most of the previous numerical studies on particle transport and deposition in human respiratory system were limited to the inner tracks while the external conditions outside of the respiratory tracts were rarely taken into account. Due to the lack of accurate information about the velocity profiles on the inlet of the respiratory tracts (e.g. the nostrils or the mouth), uniform velocity boundary conditions were generally employed instead in these studies. This simplification may lead to obvious uncertainty or inaccuracy in translation of the findings back to real life. In fact, some existing investigations have found that both the structures (ge, 2012; Inthavong, Wen, et al., 2008) and the airflow conditions (King Se, Inthavong, et al., 2010) outside the human respiratory system have significant effects on the airflow dynamics and particle transport patterns within it.

In order that the effects of external conditions on particle deposition in respiratory tracts could be effectively characterized, CFD simulations of particle transport and deposition in a human nasal cavity were conducted by the authors (Li, Inthavong, et al., 2012), using two types of inlet velocity profiles at the nostrils, respectively. One type was the widely used uniform inlet velocity profile while the other was a realistic inlet velocity profile which was obtained through a separate CFD computation of particle inhalation by a human manikin from a typical indoor environment. It was revealed that the external structures (e.g. the manikin facial features) led to a complicated and non-uniform velocity profile at the nostril openings. This discrepancy further led to different predictions of airflow fields and local particle deposition efficiency in the nasal cavity, especially in the anterior regions. It was therefore concluded that for CFD simulations of particle deposition in the nasal cavity, the inlet velocity profiles induced by external conditions are important for more realistic results.

However, this two-step numerical procedure also suffers from information loss when translating velocity profiles from one CFD model to another. This study extended the previous investigations by simulating simultaneously the processes of particle inhalation from the ambient environment and particle deposition in the nasal cavity, using an integrated human manikin model which includes detailed facial features and a realistic nasal cavity. Details visualization results including velocity vectors, particle tracks and particle inhalability and deposition rate were

obtained. Compared with the previous CFD models, the integrated model in this study, although more cost expensive, is believed to be more effective in capturing the factors in the ambient environment affecting particle inhalation and deposition.

NUMERICAL PROCEDURES

Computational models

The computational domain is illustrated in Figure 1, which represents a ventilated room containing a standing breathing human manikin (1.70 m height) at its central plane. The dimensions of the room (4m-width \times 10m-depth \times 3m-height) are created large enough so that the flow field near the manikin is free from the effects of the no-slip condition of the stationary surrounding walls. In order that the effects of both facial structures and ambient airflow on particle transport in the nasal cavity could be taken into account, the manikin is built to be integrated

which includes detailed facial features and a realistic nasal cavity. The manikin structures outside and inside the respiratory tracts are connected through the nostrils. In this study, both the facial features and the nasal geometry were reconstructed using the commercial grid generator ICEM-CFD (Ansys Inc.) based on CT scans of a healthy, 28-year old Asian male volunteer, 170 cm height, 75 kg. The computational domain is filled with unstructured tetrahedral elements, with finer elements employed in the nasal cavity and other complicated or narrow zones such as the nose and the mouth. In addition, a near-wall region consisting of dense prism layer elements was generated in order to capture the near-wall airflow/particle behaviours. The mesh-independency was achieved at 11.6 million cells. The final plane mesh structures inside the nasal cavity are also shown in Figure 1.

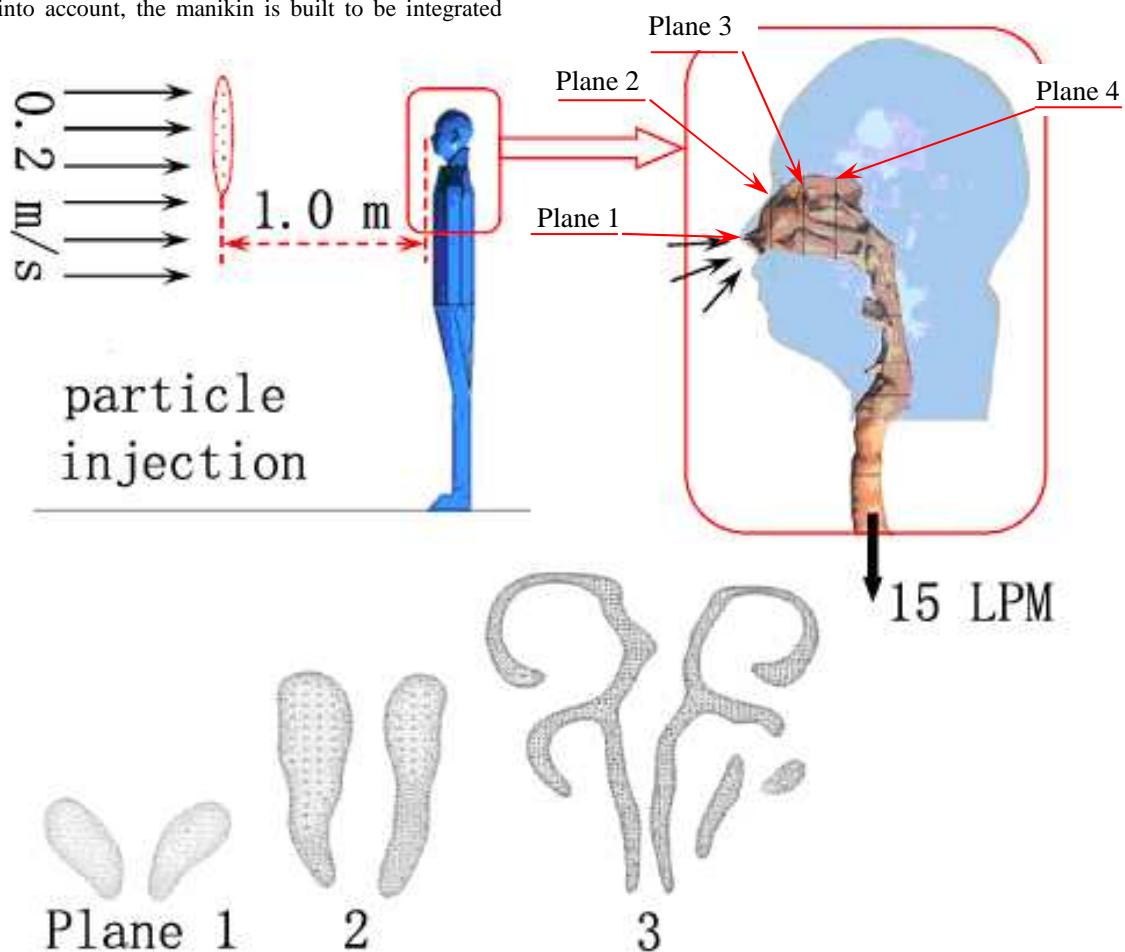


Figure 1: The integrated computational model.

Modelling of fluid flow

The free stream velocity is arranged to be normal to the face, which is referred to as “facing-the-wind” flow direction. A uniform free stream of 0.2 m/s representing an average wind speed in most indoor environment (Baldwin and Maynard 1998) is applied at the domain inlet. An opening boundary condition is applied at the opposite side of the room so that mass conservation could be maintained in the whole computational domain. The periodic

respiratory activity of a realistic human body was ignored and a constant inhalation rate of 15 litres per minute (LPM) representing a light breath at resting status is applied at the out of respiratory tracts. The steady, incompressible Navier-Stokes equations are solved for the airflow. The continuity and momentum equations are given in Eq. (1) and (2) respectively.

$$\nabla \cdot (\rho \bar{U}) = 0 \quad (1)$$

$$\begin{aligned} & \nabla \cdot (\rho \bar{U} \otimes \bar{U}) \\ & = \nabla \cdot (\mu + \mu_t) \left(\nabla \bar{U} + (\nabla \bar{U})^T - \frac{2}{3} \delta_{ij} \nabla \cdot \bar{U} \right) - \nabla p \end{aligned} \quad (2)$$

To resolve the boundary layer in the near wall regions, the Scalable Wall Function (Mühlfeld, Gehr et al. 2008) was used. The pressure-velocity coupling was resolved using the SIMPLEC algorithm. The convective terms of the transport equations were discretized using second-order-upwind scheme in order to obtain sufficiently accurate solutions. The fluid flow equations were solved in ANSYS CFX 12.1 using a segregated solver with an implicit formulation.

Modelling of particle transport

Particles with density of 1000 kg/m^3 representing water drops are released from a circular plane 1.0 m upstream of the nose tip (Figure 1). The particle size is chosen to be small enough (1.0 micron) so that the gravitational and inertial effects on particle movement are very weak and their transport is mainly controlled by the airflow field. The diameter of the circular particle injection region is 0.4 m. To achieve a uniform particle concentration assumption, the particles were released at the same velocity as that of the free stream (0.3 m/s). The number of injected particles was checked for statistical independence. It was found that independence was achieved at 50,000 particles since a further increase to 100,000 particles yielded a difference less than 0.1% in the particle deposition efficiency in the nasal cavity.

The particles are tracked through the continuum fluid separately using the Lagrangian approach and the equation of particle motion is given by

$$m_p \frac{d\bar{U}_p}{dt} = \bar{F}_D + \bar{F}_B \quad (3)$$

The drag force \bar{F}_D and buoyancy force \bar{F}_B are defined by, respectively

$$\bar{F}_D = \frac{1}{2} C_D \rho A_p |\bar{U} - \bar{U}_p| (\bar{U} - \bar{U}_p) \quad (4)$$

$$\bar{F}_B = (m_p - m) \bar{g} = \frac{\pi}{6} d_p^3 (\rho_p - \rho) \bar{g} \quad (5)$$

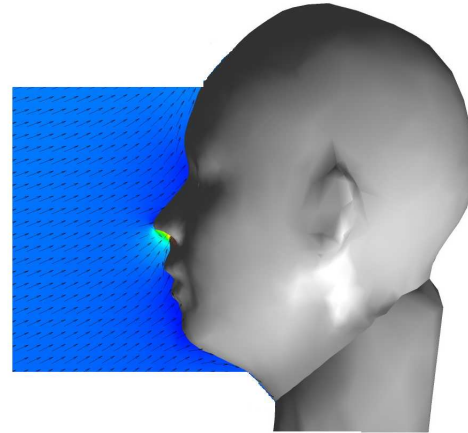
Particles are assumed to rebound when hitting the manikin surface while they are captured when they hit the respiratory tract walls. Details of the Lagrangian particle modelling have been highlighted in our previous study (King Se, Inthavong et al. 2010) and will not be repeated here.

RESULTS AND DISCUSSION

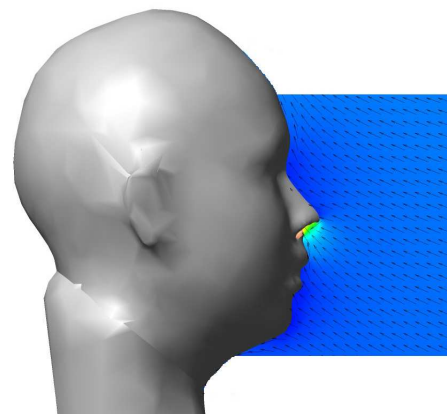
Airflow field

Our previous study (Se, Inthavong et al. 2010) has demonstrated that no matter for mouth inhalation or nasal inhalation, the airflow velocity profile at the inlet of human respiratory tracts are very complicated since the airflow bend sharply to avoid the obstacle of solid facial features. This study further supports this conclusion. As illustrated in Figure 2, as the airflow approaching the nostrils, it bends its way towards while accelerates to flow into the nostrils. In terms of the side views (Figure 2 (a) and (b)), it is clear that the airflow bends its way upwards before entering the nostrils, which leads to an increased

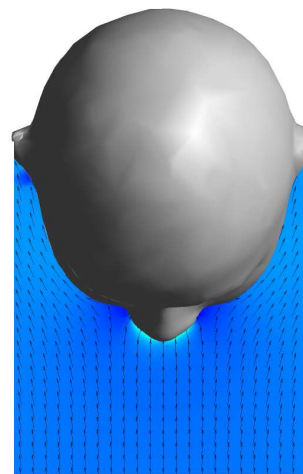
flow intensity and complicated velocity profile at the nostrils. According to the top view (Figure 2 (c)), it is found that the airflows entering both nostrils are pointing to the nose bridge (Li, Inthavong et al. 2012), which may lead to a significant particle deposition in the vestibule region due to particle collision with the airway walls.



(a) Left view



(b) Right view



(c) Top view

Figure 2: Airflow field in the breathing zone.

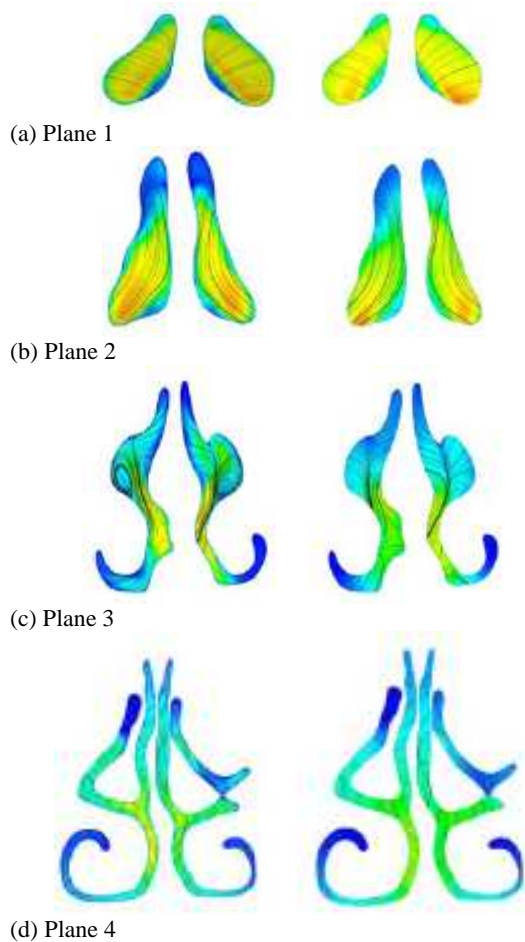


Figure 3: Airflow field in the nasal cavity.

As a result of the complicated airflow velocity profile at the nostrils, the airflow velocity is found to be unevenly distributed within the whole nasal cavity. Figure 3 illustrates two-dimensional airflow fields in the cross-planes (Figure 1). For the purpose of comparison, airflow fields in the same planes yielded from a separate computation using uniform inlet velocity profile at the nostrils are also presented. It was found that the integrated model yielded a stronger vortex flow in the nasal cavity, especially in the anterior parts such as the vestibule and valve regions. The difference in airflow field decreases with increased distance from the nostrils. At plane 4, the airflow field distributions are almost the same despite the different boundary conditions. This indicates that the velocity profile at the nostrils has a significant effect on the airflow in the interior of nasal cavity. This effect will inevitably lead to different prediction of particle deposition pattern in the nasal cavity.

Particle tracks

Figure 4 illustrates the tracks of inhaled particles. It was found that before entering the respiratory tracts, the particles bend their ways in fit the geometric shape the nostrils, which leads to a complicated particle velocity profile at the inlet of the respiratory tracts. In fact, a comparison of Figure 4 against Figure 2 demonstrates that the particle tracks have a very similar distribution to that of the airflow, this is because of the flow-controlled particle transport due to the small particle size. As a result

of the complicated particle velocity at the nostrils, the particle transport and deposition patterns in the nasal cavity are also significantly changed.

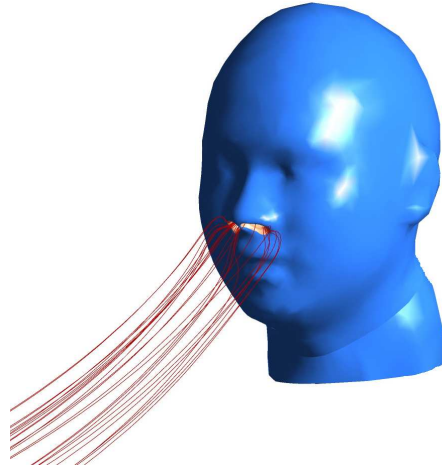
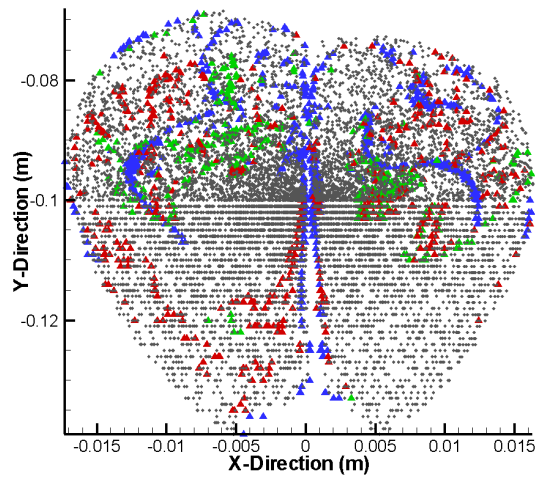


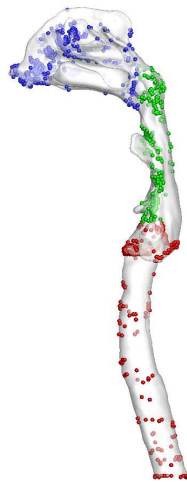
Figure 4: Tracks of inhaled particles.

Our previous study (Li, Inthavong et al. 2012) has proved that a uniform particle velocity boundary condition at the nostrils would lead to an under-predicted particle deposition efficiency in the nasal cavity. In this study, this particle deposition is analysed together with the process of particle inhalation using the concept of “critical area” proposed by Anthony (Anthony and Flynn 2006). Figure 5 (a) presents the critical area which is located in the particle injection plane while Figure 5(b) presents the particle deposition pattern in the respiratory tracks. The coordinate original point (0, 0, 0) in Figure 5 locates on the nose tip of the manikin (Figure 1). In Figure 5, blue particles deposit in the nasal cavity region, green particles deposit in the laryngopharynx region, red particle deposit in the trachea region and grey particles go further into the lung. It was found according to Figure 5(a) that the inhaled particles are actually released from a small area (7cm-height \times 4cm-width) lower than the nostrils. However, the particle deposition in the respiratory tracts seems not relevant to the release location within the critical area since particles with different colours are randomly distributed in the critical area. The particle deposition efficiency in different regions of the respiratory tracts is also analysed. For the issue in this study, most of the inhaled particles (93.3%) are transported into the lung while a small portion (6.7%) deposit in the tracts. Within the 6.7% deposited particles, over half of them (3.5%) deposit in the nasal cavity due to its complicated geometrical structure and airflow pattern.

When compared with the previous studies which investigate particle inhalation and deposition separately, the integrated simulation of particle inhalation from the ambient environment and particle deposition in the respiratory tracts presents a comprehensive method for the assessment of health risks associated with particle inhalation since it not only locates the source of inhaled particles, but also tell which local region these particles deposit. The particles can be reversely tracked from their deposition positions to their release locations. More importantly, this integrated method eliminates unnecessary information loss of the velocity profile at the nostrils due to data translation.



(a) Critical area



(b) Particle deposition pattern in the respiratory tracts

Figure 5: Particle inhalation critical area and deposition pattern. (Blue = 3.5%; Green = 1.4%; Red = 1.8%; Gray = 93.3%).

CONCLUSION

The process of particle inhalation from the ambient environment and deposition in human respiratory tracts are numerically investigated using an integrated human manikin model. Detailed results including airflow field, particle tracks and deposition pattern are obtained and compared against our previous results obtained through separate simulations. Conclusions arising from this study are as follows:

- (1) The integrated model yielded a stronger vortex flow in the nasal cavity, while the flow in the laryngopharynx and trachea regions is not significantly affected.
- (2) The velocity profile at the nostrils is very complicated and subjected to the structures and flow conditions outside the respiratory tracts. The effects of these external factors have to be taken into account for the purpose of accurate prediction.
- (3) The integrated model of this study provides a comprehensive method for assessment of health risk associated with particle inhalation and deposition.

ACKNOWLEDGEMENTS

The financial supports provided by the Australian

Research Council (project ID LP110100140) and by the National Basic Research Program (973) of China (Grant No. 2012CB720100) are gratefully acknowledged.

REFERENCES

- ANTHONY, T.R. and FLYNN, M.R., (2006), "Computational fluid dynamics investigation of particle inhalability", *J Aeros. Sci.*, **37**, 750-765.
- BALDWIN, P.E.J. and MAYNARD, A.D., (1998), "A survey of wind speeds in indoor workplaces", *Ann. Occup. Hyg.*, **42**, 303-313.
- DOORLY, D.J., TAYLOR, D.J., et al., (2008), "Mechanics of airflow in the human nasal airways", *Resp. Phys. & Neur.*, **163**, 100-110.
- GE, Q., (2012), *Numerical studies of particle inhalation into human respiratory system*, PhD, RMIT University.
- INTHAVONG, K., WEN, H., et al., (2008), "Numerical study of fibre deposition in a human nasal cavity", *J Aeros. Sci.*, **39**, 253-265.
- KING SE, C. M., INTHAVONG, K., et al., (2010), "Inhalability of micron particles through the nose and mouth", *Inhal. Toxi.*, **22**, 287-300.
- LI, X. D., INTHAVONG, K., et al., (2012), "Particle inhalation and deposition in a human nasal cavity from the external surrounding environment", *Build. Envi.*, **47**: 32-39.
- LIU, Y.A., MATIDA, E.A., et al, (2010), "Experimental measurements and computational modeling of aerosol deposition in the Carleton-Civic standardized human nasal cavity", *J Aero. Sci.*, **41**, 569-586.
- MUHLFELD, C., GEHR, P., et al., (2008), "Translocation and cellular entering mechanisms of nanoparticles entering mechanisms of nanoparticles", *Swiss Medical Weekly*, **138**, 256-266
- SHI, H.A., KLEINSTREUER, C., et al., (2007), "Modeling of inertial particle transport and deposition in human nasal cavities with wall roughness." *J Aero. Sci.*, **38**, 398-419.
- STOREY-BISHOFF, J., NOGA, M., et al, (2008), "Deposition of micrometer-sized aerosol particles in infant nasal airway replicas." *J Aero. Sci.*, **39**, 1055-1065.